Possible Detection of Cyclotron Resonance Scattering Emission Features from an Accretion-powered Pulsar 4U 1626−67

Wataru Iwakiri[1] Yukikatsu Terada[1] Makoto.S.Tashiro[1]
Tatehiro Mihara[2] Kazuo Makishima[3] Teruaki Enoto[3]
Motoki Nakajima[4] Atsumasa Yoshida[5] and Lorella Angelini[6]

[1] Saitama University, 255 Shimo-Okubo, Sakura, Saitama, 338-8570, Japan
[2] Institute of Physical and Chemical Research (RIKEN), 2-1 Hirosawa, Wako, Saitama 351-0198, Japan
[3] University of Tokyo, 7-3-1 Hongo, Bunkyo, Tokyo, 113-0033, Japan
[4] Nihon University, 2-870-1 Sakaemachi-Nishi, Matsudo, Chiba, 271-8587, Japan
[5] Aoyama Gakuin University, 5-10-1 Fuchinobe, Sagamihara, 229-8558, Japan
[6] Laboratory for High Energy Astrophysics, NASA Goddard Space Flight Center, Code 660, Greenbelt, MD 20771
E-mail(WI):iwakiri@crystal.heal.phy.saitama-u.ac.jp

Abstract

The presenting paper summarizes the *Suzaku* observation of the low-mass X-ray binaries 4U 1626−67 showing 7.7 s pulsation. Thanks to the high sensitivity of the Hard X-ray Detector (HXD), are clearly detected the Cyclotron resonance scattering features (CRSFs) at 37 keV with 88 ks exposure in March 2006. The feature is consistent with the value measured by *BeppoSAX* (Orlandini et al.1998), and an emission line feature at the cyclotron resonance energy is possibly detected in a dim phase. the bright phases, obtained spectra above 3 keV are well reproduced by Negative and Positive power-law times exponential cutoff (NPEX) model multiplied by a fundamental CRSF. On the other hand, the phase-resolved spectra in the dim phase does not show Wien peak, and the CRSFs can be reproduced by either emission line model or absorption model. The spectrul properties in the dim phase in comparison with these in other phases and theoritical spectrum, imply that the CRSF is an emission feature rather than an absorption feature.

Key words: CRSFs,Wien peak,Emission feature

1. Introduction

The Cyclotron Resonance Scattering Features (CRSFs) were first discovered in the hard X-ray spectrum of Her X-1 (Trümper et al.1978). The effects are caused by resonant scatterings of photons by electrons in Landau level under a storng magnetic field near the neutron star surface. Recently, CRSFs have been observed in more than 16 X-ray pulsars (Mihara 1995; Coburn et al.2002), only with absorption features. Their line energies, profiles and width all depend on the details of emission, electron temperature, optical depth and viewing geometries, therefore CRSFs carry a infomation of plasma emissions and their radiative transfer in the accretion column on the magnetic pole.

4U 1626−67 is a low-mass X-ray binary consisting a neutron star with a spin period of 7.7 s. The CRSFs from this object discovered at 37 keV as an absorption feature by *BeppoSAX* (Orlandini et al.1998). The X-ray continuum has strong phase dependence as reported by *HEAO-1* (Pravdo et al.1979), and *RXTE* (Coburn et al.2002). In addition, *RXTE* has shows a hint of a variability of CRSFs. In order to study the variability of the X-ray spectra, including the continuum and the CRSFs, we performed the high sensitive X-ray observation of 4U 1626−67 with *Suzaku* in 2006. Here, in this paper, we summraize the results of this observation.

2. Observation and data reduction

2.1. Suzaku observation of 4U1626-67

The fifth Japanese X-ray satellite *Suzaku* (Mitsuda et al.2007) which carries on board the two instruments. The first is the X-ray Imaging Spectrometer (XIS; Koyama et al.2007) covering energy range of 0.2 - 12 keV. Three (XIS0, XIS2 and XIS3) of the XIS chips are front-illuminated (FI) CCDs, while XIS1 utilizes a back-illuminated (BI) one. The second is the Hard X-ray Detector (HXD; Takahashi et al.2007) which covers the 10 - 70 keV with p-i-n types silicon diodes (HXD-PIN) and the 50 - 600 keV with Gd_2SiO_5Ce (GSO) scintillators. We observed 4U1626−67 with *Suzaku* on 2006

March 9 UT 01:18 through March 11 19:38. The observation carried out at the "XIS nominal" pointing position, for a net exposure of 102.7 ks with the XIS and 87.6 ks with the HXD. The XIS operated in normal mode with the "1/8 window" option to improve the time resolution to 1 s, without charge injection function.

2.2. Data reduction

We used the datasets produced by the Suzaku pipeline processing version 2.0.6.13 with the calibration version of hxd-20090515, xis-20090403 and xrt-20080709, using tools in the HEADAS package 6.5.1. We used the XSPEC version 12.4.0 to fit spectra with models.

In the XIS analysis, we screened the data by the standared criteria; we discarded the events when the elevation above Earth's limb was below 5°, Earth's day-night boundary was less than 25°, or the spacecraft was in, and 436 s after, leaving the South Atrantic Anormaly (SAA). Then we selected events within 6 mm (4'.3) of the image centroid. The intensity of XIS in the 0.4 - 10.0 keV band is about 5 c s^{-1} per sensor. The XIS backgrounds were taken from a source free region of the corresponding sensor. The derived background, exhibiting a rate of 0.02 c s^{-1}per sensor in 0.4 - 10.0 keV, is generally negligible. The HXD data was also screened by the standard criteria; we discaded the data within the same time interval an that of the XIS, but within 500 s after the passage of SAA.The non X-ray background (NXB) of HXD-PIN was calculated as simulated photon data, whose model parameters were continuously tuned using the Earth occultation data (LCFITDT in `Fukazawa et al.2009` and version of METHODV = 2.0). This NXB was reported to have a systematic reproducibility error of 2.31% with 10 ks exposure, respectively, in the 15 - 40 keV. We faked the cosmic X-ray background (CXB) spectra as following the *HEAO-1* results `(Boldt 1987)`. Then, we employed the PIN-background which is added NXB and CXB.

3. Analysis and Results

3.1. Timing Analysis

To determine the pulse period of the *Suzaku* observation, we correct the arrival times of the XIS and PIN events of orbital motion effect of the Earth around the sun, and that of the satellite around the Earth using aebarycen `(Terada et al.2008)`. After the barycentric correction, the pulse period has been determined as $P_{(\mathrm{suzaku})}$=7.67795(9) sec. The result is roughly consistent with a spin-down trend started in 1990.

Fig.1 shows energy sorted, background-inclusive pulse profiles of 4U1626-67, folded at the spin period, $P_{(\mathrm{suzaku})}$. The bottom panel shows the hardness ratio between 10 - 30 keV and 30 - 50 keV. Thus, the spectra get harder at the dim phase.

3.2. Phase-Averaged Spectra

To check the X-ray spectral shape without artificial effects of the response of instruments, we first divided them to the X-ray spectra of Crab Observation. The results of Crab ratio, shown in Fig.2 (a), indicates that the source intensity is about 30 mCrab at 20 keV. The ratio rise up with power-law shape from 3 keV to 20 keV, then falls steeply like a Wien peak into harder band. Moreover, dip features, which should be caused by cy-

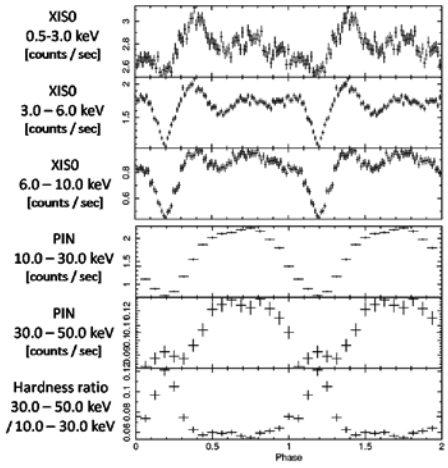

Fig. 1. Energy-sorted and background-inclusive pulse profiles of 4U 1626-67. The data were folded by the barycentric corrected pulse period, P=7.67795 s.

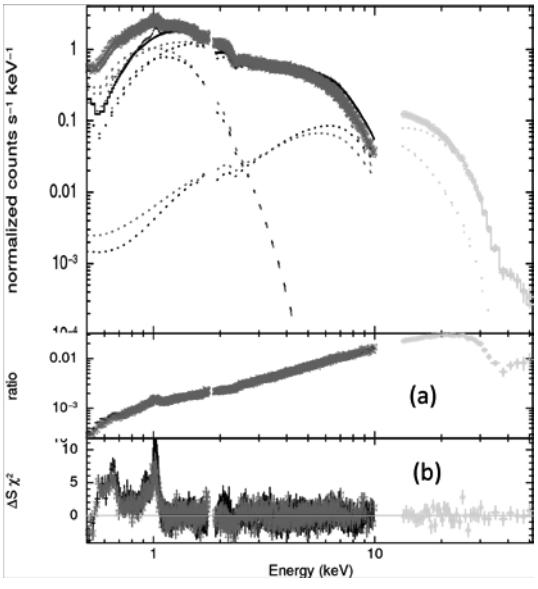

Fig. 2. Phase-averaged and back ground-subtracted spectra of 4U1626-67 obtained with the *Suzaku* XIS (black and grey) and HXD (light grey). They are presented without removing instrumental responses, and error bars show statistical only. (a) Same spectra divided by those of Crab nebula. (b) Residuals from a blackbody plus NPEX and Gaussian-absorption model with the photo electric absorption.

clotron resonance scattering around 35 keV, are clearly seen. Since the continuum shape is similar to an unsaturated thermal Comptonization (e.g., Mészáros 1992; Sunyaev Titarchuk 1980), we employed the Negative and Positive power-law times EXponetial model (so called NPEX model; Mihara 1995; Makishima et al.1999) in the model fitting of the spectra;

$$f(E) = (A_n E^{-\alpha} + A_p E^{+\beta}) \times \exp\left(-\frac{E}{kT}\right). \qquad (1)$$

where E is the energy of incident photon, $f(E)$ is the photon number spectrum, T is a plasma temperature (thus, kT is the cutoff energy). The negative term describes power-law shape at low energy side. As the energy increases, the positive term, which simulates the Wien peak in a saturated Comptonization when $\beta = 2.0$, becomes dominant. We fitted the data by a blackbody plus NPEX and Gaussian-absorption model (GABS; Kreykenbohm 2004) with the photo electric absorption. The results are presented in Fig 2. Since the blackbody component is less than 1 % as compared with NPEX's negative term at 3 keV, we fitted the data only above 3 keV by NPEX mutiplied Gaussian-absorption model, and got best fit parameters summrized in table 1.

3.3. Phase-Resolved Spectra

As reported by *HEAO-1* and *RXTE* (Pravdo et al.1979; Coburn et al.2002), the object shows a strong phase dependence in the continuum emission, thus we further checked its phase-resolved spectra with *suzaku*. We divided events into eight epochs. Fig.3 shows the phase-resolved Crab ratio in these epochs. The two facts appear in Fig.3; First, the Wien peak gets weaker as the flux falls. Second, the resonance feature seems to be variant in each phase. The second point is strongly appeared at the dim phase ($\phi = 0.125$ - 0.250). We tried the NPEX with the Gaussian absorption model, as presented in the phase-averaged analysis in the previous section, to represent the phase-resolved spectra except for dim phase. The results are summarized table 2. We fitted the dim phase spectra only by NPEX. No finite value of A_p is required; this fact implies that the spectrum does not has Wien peak. The fitting is acceptable, however, still some feature around 30 keV remains as presented in Fig.4 (a). To describe the feature, we tried two models; NPEX plus Gaussian emission model or NPEX with Gaussian absorption, as presented in the phase-averaged spectal analysis. If we take the former model, the residual feature dessapered with F-test significance of about 3 sigma. If we take the latter model, the fitting is also acceptable, however, the value of kT obtained from the absorption model is not consistent with those in other phases. On the other hand, in the emission case, the kT was consistent with the value of the other phases.

4. Discussion

We found a possible cyclotron resonance emission feature in the X-ray spectrum at the dim phase of 4U 1626−67. Fig.5 shows the unfolded spectra of on-phase ($\phi = 0.625 - 0.750$) and dim phase ($\phi = 0.125 - 0.250$). This observational results are similar to the theoritical spectrum of magnetized slab of Thomson optical depth between 1 and 10 caluculated by Nagel (Nagel et al. 1981b); the Wien peak disappers with appearrance of emission like feature. Therefore, we may conclude that the dim phase feature is caused by cyclotron resonance scatering rather than absorption. This transition seems to be appeared as the object rotates. Detailed discussion will be described in a separate paper.

5. ACKNOWLEDEMENT

We thank all of the *Suzaku* team members for their dedicated support of the satellite operation and calibration.

References

Boldt, E. 1987, Observational Cosmology, 124, 611
Coburn, W., et al. 2002, ApJ ,580, 394
Fukazawa, Y., et al. 2009, PASJ, 61, 17

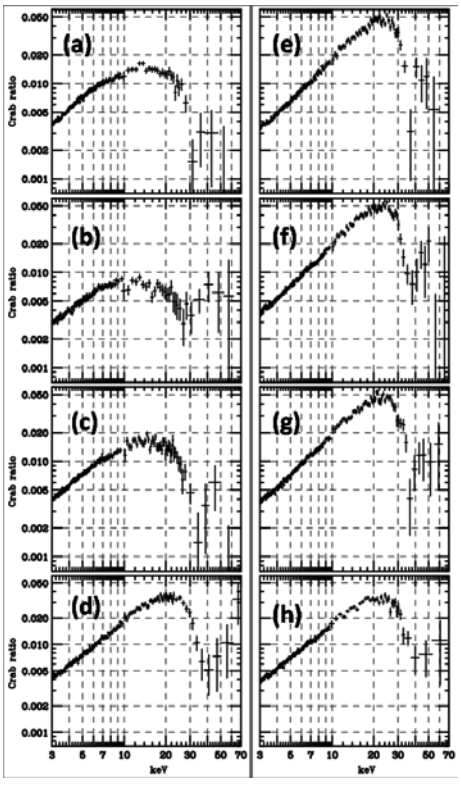

Fig. 3. Ratios of the phase-resolved and backgroun-subtrcted XIS and HXD spectra of 4U 1626-67 to those of the Crab Nebula. (a) $\phi = 0.000-0.125$. (b) $\phi = 0.125-0.250$. (c) $\phi = 0.250-0.375$. (d) $\phi = 0.375 - 0.500$. (e) $\phi = 0.500 - 0.625$. (f) $\phi = 0.625-0.750$. (g) $\phi = 0.750-0.875$. (h) $\phi = 0.875-1.000$.

Table 1. Best fit parameters of phase averaged spectra of 4U 1626-67 above 3 keV.

α	β	kT[keV]	$A_n(\times10^{-3})$	$A_p(\times10^{-5})$	E_a[keV]	σ [keV]	τ	χ^2 / d.o.f
$0.34^{+0.02}_{-0.01}$	-2.00(fix)	$6.08^{+0.19}_{-0.16}$	$8.09^{+0.22}_{-0.22}$	$3.07^{+0.38}_{-0.42}$	$36.6^{+0.9}_{-0.8}$	$4.37^{+0.63}_{-0.56}$	$14.6^{+3.0}_{-2.4}$	580 / 513

Table 2. Best fit parameters of phase resolved spectra of 4U 1626-67 above 3 keV. (a) Fit parameters when only an NPEX ($A_p = 0$) continuum is fitted. (b) Fit parameters from the NPEX ($A_p = 0$) + Gaussian. (c) Fit parameters from the NPEX ($A_p = 0$) × GABS.

phase	α	kT [keV]	$A_n(\times10^{-3})$	$A_p(\times10^{-5})$	E_a[keV]	σ [keV]	τ	χ^2 / d.o.f
0.125-0.250 (a)	$0.28^{+0.7}_{-0.07}$	$6.45^{+0.42}_{-0.39}$	$6.13^{+0.38}_{-0.36}$	0				133 / 124
0.125-0.250 (b)	$0.26^{+0.07}_{-0.08}$	$6.22^{+0.44}_{-0.49}$	$5.99^{+0.39}_{-0.39}$	0	$41.4^{+14.9}_{-5.0}$	$7.05^{+\infty}_{-4.58}$	$5.41^{+7.16}_{-2.85}$	118 / 118
0.125-0.250 (c)	$0.56^{+0.11}_{-0.14}$	$14.2^{+4.4}_{-3.8}$	$7.01^{+0.81}_{-0.53}$	0	$26.9^{+3.7}_{-3.4}$	$14.2^{+3.8}_{-2.9}$	$14.2^{+36.2}_{-20.4}$	111 / 118
0.000-0.125	$-0.20^{+0.05}_{-0.05}$	$7.27^{+0.37}_{-0.33}$	$6.45^{+0.33}_{-0.30}$	0	$31.3^{+2.3}_{-1.6}$	$0.57^{+11.16}_{-0.31}$	$54465.3^{+\infty}_{-54459.8}$	102 / 129
0.250-0.375	$0.36^{+0.07}_{-0.06}$	$8.81^{+1.10}_{-0.60}$	$7.96^{+0.45}_{-0.40}$	0	$33.3^{+6.2}_{-2.6}$	$4.42^{+3.46}_{-1.81}$	$15.0^{+23.7}_{-7.15}$	126 / 147
0.375-0.500	$0.48^{+0.09}_{-0.05}$	$5.51^{+0.29}_{-0.25}$	$10.9^{+1.15}_{-0.86}$	$5.64^{+1.20}_{-1.13}$	$37.2^{+4.1}_{-2.1}$	$4.23^{+2.52}_{-1.65}$	$14.9^{+14.3}_{-6.17}$	131 / 155
0.500-0.625	$0.46^{+0.07}_{-0.05}$	$6.36^{+0.32}_{-0.28}$	$8.11^{+0.77}_{-0.66}$	$4.35^{+0.85}_{-0.77}$	$36.9^{+1.7}_{-1.2}$	$3.77^{+1.12}_{-1.13}$	$19.5^{+7.8}_{-5.2}$	146 / 146
0.625-0.750	$0.49^{+0.05}_{-0.06}$	$6.19^{+0.26}_{-0.18}$	$9.37^{+0.62}_{-0.80}$	$5.13^{+0.64}_{-0.99}$	$36.4^{+1.3}_{-0.7}$	$3.76^{+0.97}_{-0.73}$	$18.5^{+6.8}_{-3.5}$	145 / 159
0.750-0.875	$0.40^{+0.06}_{-0.06}$	$6.44^{+0.55}_{-0.27}$	$8.20^{+0.72}_{-0.65}$	$4.16^{+0.86}_{-1.17}$	$37.9^{+2.8}_{-1.4}$	$4.83^{+1.28}_{-0.96}$	$21.7^{+10.4}_{-5.7}$	177 / 157
0.875-1.000	$0.43^{+0.07}_{-0.05}$	$6.00^{+0.43}_{-0.53}$	$9.23^{+1.21}_{-0.84}$	$3.91^{+1.63}_{3.28}$	$41.6^{+15.5}_{-5.8}$	$7.27^{+12.65}_{-5.52}$	$20.2^{+201.6}_{-14.6}$	138/ 159

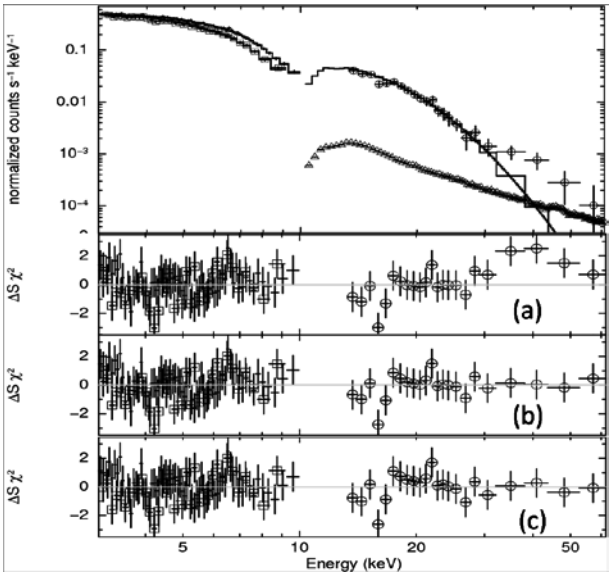

Fig. 4. The upper panel shows the dim phase (ϕ = 0.125-0.250) spectra of 4U 1626-67 with the Suzaku XIS (crosses and square) and HXD (circle). The triangle show the reproducibility of NXB. The histgrams in the upper panel are NPEX continuum ($A_p = 0$). (a) Residuals when only an NPEX ($A_p = 0$) continuum is fitted. (b) Fit residuals from the NPEX ($A_p = 0$) + Gaussian. (c) Fit residuals from the NPEX ($A_p = 0$) × GABS.

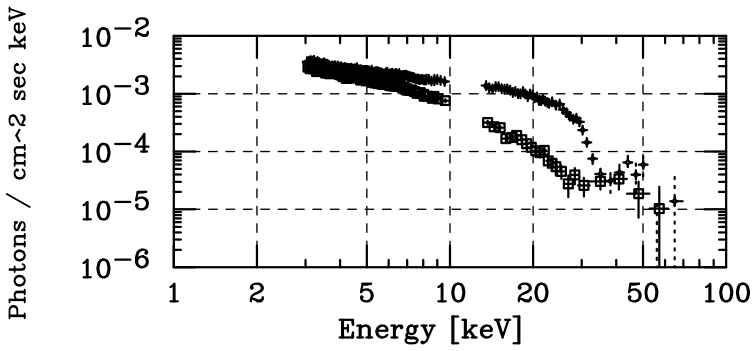

Fig. 5. The unfolded spectrum of 4U1626−67. The crosses shows on-phase spectra($\phi = 0.625 - 0.750$). The squares shows off-phase spectra($\phi = 0.125 - 0.250$).

Koyama, K., et al. 2007, PASJ, 59, S23
Kreykenbohm,I., Wilms,J., Coburn,W., Kusuter,M., Rothschild,R.E., Helindl, W.A., Kretschmar, P., Staubert, R. 2004, AA, 427, 975
Makishima, K., et al. 1999, ApJ, 525, 978
Mészáros, P. 1992, High Energy Radiation from Magnetized Neutron Stars (Chicago:Univ.of Chicago Press)
Mihara, T. 1995, Ph.D.thesis, Dept.of Physics, Univ. of Tokyo
Mitsuda, K., et al. 2007, PASJ, 59, S1
Nagel, W., et al. 1981, ApJ, 251, 288
Orlandini, M., et al. 1998, ApJ, 500, L163
Pravdo, S. H., et al. 1979, ApJ, 231, 912
Sunyaev,R.A., Titarchuk, L.G. 1980, AA, 86, 121
Takahashi, T., et al. 2007, PASJ, 59, S35
Terada, Y., et al. 2008, PASJ, 60, S25
Trümper, J., et al. 1978, ApJ ,219, L105